

Lawrence Berkeley National Laboratory

LBL Publications

Title

Advances and challenges in multiscale characterizations and analyses for battery materials

Permalink

<https://escholarship.org/uc/item/8sr6f5jc>

Journal

Journal of Materials Research, 37(19)

ISSN

0884-2914

Authors

Bianchini, Matteo
Lacivita, Valentina
Seo, Dong-Hwa
[et al.](#)

Publication Date

2022-10-14

DOI

10.1557/s43578-022-00743-7

Copyright Information

This work is made available under the terms of a Creative Commons Attribution-NonCommercial-ShareAlike License, available at <https://creativecommons.org/licenses/by-nc-sa/4.0/>

Peer reviewed

Advances and Challenges in Multi-scale Characterizations and Analyses for Battery Materials

Matteo Bianchini,^{1#} Valentina Lacivita,^{2#} Dong-Hwa Seo,^{3#} Haegyeom Kim^{4*}

1. Universität Bayreuth, Universitätsstraße 30, D-95447 Bayreuth, Germany
2. Advanced Materials Lab, Samsung Semiconductor, Inc., Cambridge MA 02138, USA
3. School of Energy and Chemical Engineering, Ulsan National Institute of Science and Technology (UNIST), Ulsan 44919, Republic of Korea
4. Materials Sciences Division, Lawrence Berkeley National Laboratory, Berkeley 94720, USA

#These authors contributed to this work equally.

*Corresponding author: haegyumkim@lbl.gov

Keywords: Energy Storage; Multiscale; Crystallographic Structure; Microstructure; Modeling

Abstract

Rechargeable ion batteries are efficient energy storage devices widely employed in portable to large-scale applications such as electric vehicles and grids. Electrochemical reactions within batteries are complex phenomena and they are strongly dependent on the battery materials and systems used. These electrochemical reactions often include detrimental irreversible reactions at various length scales from atomic- to macro-scales, which ultimately determine the overall electrochemical behavior of the system. Understanding such reaction mechanisms is a critical component to improve battery performance. To help this effort, this review article discusses recent advances and remaining challenges in both computational and experimental approaches to better understand dynamic electrochemical reactions in batteries across multiple length scales. Important related findings from this focus issue will also be highlighted. The aim of our focus issue is to contribute to the battery community towards having better understanding of complex reactions occurring in battery devices and of computational and experimental methods to investigate them.

Introduction

Decarbonization and electrification are becoming priority topics in the modern society because of the growing concern on the global climate crisis, resulting from significantly increasing energy consumption. The U. S. targets to address the climate crisis by achieving net-zero emissions of carbon dioxide (CO₂) by 2050.^{1, 2} Electrochemical energy storage is one of the most efficient ways to utilize renewable energy sources, e.g., solar, wind and geothermal energy.³ Lithium (Li)-ion batteries (LIBs) have been successful to electrify portable devices because of their high energy density, and now their applications expand to larger scales such as electric vehicles and grids. For those large scale applications, the U. S. Department of Energy (DOE) established an important target, the *Long Duration Storage Shot*, to reduce the cost of grid-scale energy storage by 90% for systems that deliver more than 10 hours of duration within a decade.¹ In this respect, beyond LIB technologies, such as sodium (Na)-, potassium (K)-, and magnesium (Mg)-ion batteries, have been considered as alternative energy storage systems because they are based on abundant elements, including intercalation ions (Na, K, and Mg) and redox active elements (Co- and Ni-free cathodes).⁴⁻⁷ A recent review article in our focus issue provides an overview of positive electrode materials development for Na-ion batteries, particularly focusing on polyanion compounds.⁸

Electrochemical reactions within batteries are complicated phenomena that strongly depend on the battery materials and systems considered. They often include undesired irreversible reactions at different length scales, spanning from atomic- to macro-scales, which significantly affect their overall performance and cycle life. For example, in layered oxide cathodes, an irreversible phase transition to a spinel-like or disordered rock-salt phase at the surface during high voltage charging hinders the transport of Li ions, thereby increasing the impedance of the battery cell.⁹⁻¹¹ Often, irreversible oxygen (O₂) evolution from the cathode lattice or CO₂ evolution by electrolyte decomposition degrades the cycling stability of the battery.^{12, 13} In classical liquid electrolyte

systems, and even more so in solid-state battery systems, the formation of stable interphases between both cathode/electrolyte and anode/electrolyte during charging-discharging cycles is a key challenge to overcome.^{4, 14-16} Therefore, understanding electrochemical reaction mechanisms, whether reversible desired ones or irreversible parasitic ones, is a critical component to improve battery performance. This includes determining materials degradation mechanisms occurring in parallel to such reactions. Understanding such performance degradation mechanisms will provide insights on how to mitigate them. In this respect, both computational approaches and experimental characterization have been playing crucial and complementary roles. Figure 1 provides an overview of the computational methods and experimental characterization techniques with different length scales used to understand electrochemical reaction mechanisms occurring in battery materials and devices.

In this review article, we will discuss recent progress in computations and experimental characterization techniques to understand electrochemical reaction mechanisms in rechargeable batteries. First, we will present how multi-scale modeling and simulations are employed to understand the functionality of battery materials and the related electrochemical reactions. We will also update recent progress in machine learning techniques to help materials design. Then, we will discuss the characterization techniques for rechargeable batteries across various length scales. Both *operando* and *ex situ* characterization techniques will be considered. We will use case studies to illustrate how these advanced computational and experimental techniques improve the fundamental understanding of electrochemical reaction mechanisms in LIBs and beyond LIBs. Challenges in each technique will also be briefly discussed. Finally, we will provide perspectives on how further development of advanced computations and experimental characterization techniques can accelerate materials evolution for high-performance batteries.

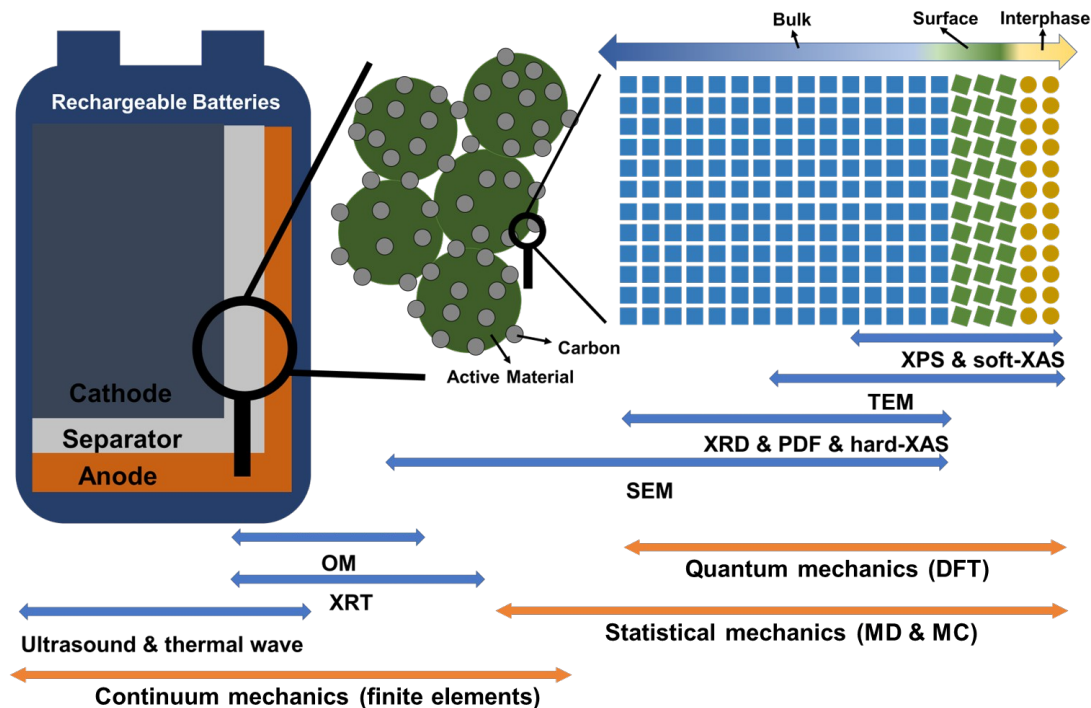


Figure 1. A schematic of the computational methods and experimental characterization techniques with different length scales to understand electrochemical reaction mechanisms.

Progress in Computations

The advancement of cost-effective rechargeable batteries requires modeling aid and ability to leverage the ever-increasing amount of available computational and experimental data. Current *in silico* research is very much focused on establishing multiscale modeling frameworks to cover all aspects of the development process, from the design of single material components up to full scale device functioning optimization. The ultimate space-time resolution in computational materials science and engineering is afforded by *ab initio* quantum mechanical (QM) approaches, usually within the Density Functional Theory (DFT). By accessing the electronic structure of materials, QM methods enable both the prediction of materials' properties and the fundamental understanding of their complex mechanisms of functioning. Indeed, the latest example is represented by the DFT work of Fasulo *et al.*¹⁷, published in this focus issue, where electric field polarization effects on TiO₂ nanoparticles are shown to favor reversible Na uptake at the (001) surface.

On the other hand, meso- to macroscopic bodies are the domain of continuum mechanics, where differentiability in space and time is assumed for all relevant physical variables and generally pursued by combining finite elements analyses with variational methods. Continuum mechanics models are an essential tool for elucidating factors limiting the battery cycle-life (including dendrites growth, microstructural degradation, and fracture propagation), and for optimizing device performance. For instance, discrete elements modeling of cathode composites in solid-state batteries has unveiled the possibility of achieving high cathode loading by controlling the size ratio between active material and conductor particles.¹⁸ In addition, in this focus issue, the review article by Sun *et al.* provides an overview of phase-field modeling in battery systems.¹⁹

For closer examinations on the state-of-the-art of both atomistic and continuum modeling of materials for battery research and their applications, the reader is referred to the numerous comprehensive and up-to-date reviews available on the subject.²⁰⁻²³ In the following, we will rather dwell on the discussion of computational methods with the potential of bridging the gap between such two extremes of the space-time scale and of facilitating the transfer of relevant knowledge or parameters from one scale to another.

Li-ion diffusion is a major factor that determines the kinetics of the charge/discharge process of electrode materials for LIBs. Therefore, it has been investigated using computational methods at various scales.²⁴⁻³⁴ The nudged elastic band (NEB) method with first-principles DFT calculation has been used to predict the minimum energy path and transition-state energy of Li-ion diffusion at atomistic scale.³⁵ For example, Morgan *et al.* reported NEB activation barriers for Li-ion diffusion in olivine-LiMPO₄ (M = Mn, Fe, Co, Ni).²⁴ They calculated activation barriers along various directions in LiMPO₄ structures and showed that the barrier along direction [010] (100-300 meV) is much lower than those along other directions (>1000 meV), which is in line with results obtained by Molecular Dynamics (MD) simulation with interatomic potentials.²⁵ This reveals that olivine LiMPO₄ cathodes have a one-dimensional Li-ion migration channel along [010] (Figure 2a), experimentally validated by combining high-temperature powder neutron diffraction and the maximum entropy method.³⁶ This channel can be blocked by Li/transition metal (TM) anti-site defects, which involve Li and TM cation mixings at M1 and M2 sites. The formation energy of the anti-site defect in LiFePO₄ is ~550 meV, estimated with DFT

calculation, which agrees with experimental observations on samples with 0.1~8% defects depending on the synthetic condition.³² TM in the lithium site blocks the lithium migration along the [010] direction and lithium cannot detour through other directions as the barriers are very high along other directions, making all Li-ions between defects along the channel inactive.

Atomistic modeling on the diffusion barriers and the anti-site defect formation energy can explain how Li-ions are blocked by the defect in LiFePO₄ qualitatively, but it cannot quantitatively explain how many lithium ions are blocked in the LiFePO₄ particle. Malik *et al.* investigated the mean fraction of unblocked lithium capacity with the particle size and the concentration of anti-site defects at macro-scale using a simple probabilistic model.³² They assumed that the anti-site defects are created with a Poisson process and located uniformly in the Li-ion channel. As all lithium located between two defects in the same Li-ion diffusion channel is blocked, they count it as a blocked capacity. Figure 2b shows the mean fraction of unblocked capacity as a function of Li-ion channel length for various defect concentrations. Even at the same defect population, there is a higher probability that the defects block more lithium ions when the particle size increases. This macro-scale simulation shows how the Li-ion diffusion in LiFePO₄ depends on particle size and defect concentration, which cannot be quantitatively studied by DFT calculations at atomic scale.

Macro-scale Li-ion diffusion in cation-disordered rock-salt (DRX) structure has also been investigated using multi-scale modeling with DFT calculation and Monte Carlo (MC) percolation simulation by Lee *et al.*³³ In a DRX Li-TM structure, both Li and TM occupy the same octahedral sites, and Li diffusion proceeds by hopping from one octahedral site to another one through an intermediate tetrahedral site (o-t-o diffusion), as shown in Figure 2c. Their DFT calculations show that the Li migration barrier of 0-TM channels, involving no face-sharing TM ions, is much lower than that of 1-TM channels involving one face-sharing TM ion in DRX cathodes. This is because Li-ions at the transitional tetrahedral site along 0-TM channels experience much weaker electrostatic repulsion than along 1-TM channels where high valent cations $M^{3+/4+/5+/6+}$ are present at face-sharing octahedra. Thus, 0-TM channels connected through the entire material, allowing Li percolation uninterrupted by 1-TM channels, are required for good Li kinetics in DRX cathodes.

However, as Li-ion and TM ions are disordered in the DRX structures, 0-TM channels are randomly distributed, making it hard to understand macro-scale Li diffusion from atomistic DFT calculation. In this respect, Lee *et al.* performed MC percolation simulations using a large supercell containing 2,048 cation sites to generate randomly distributed cations and investigate how many Li-ions percolate along 0-TM channels.^{33, 37} They estimated accessible Li content by a percolating network of 0-TM channels in DRX Li-TM oxide as a function of Li content and cation mixing (Figure 2d). More excess Li adds more 0-TM percolating network, increasing accessible Li content. This simulation can explain why stoichiometric DRX Li-TM cathodes (no Li excess) have a very low capacity, what is the minimum Li excess to activate 0-TM percolation network (percolation threshold), and what is the optimal Li excess for the largest accessible Li content. Although these macroscale simulations enable the study of macroscopic Li kinetics in cathode materials quantitatively, their results are determined by assumptions based on the understanding of Li-ion diffusion from atomistic modeling.

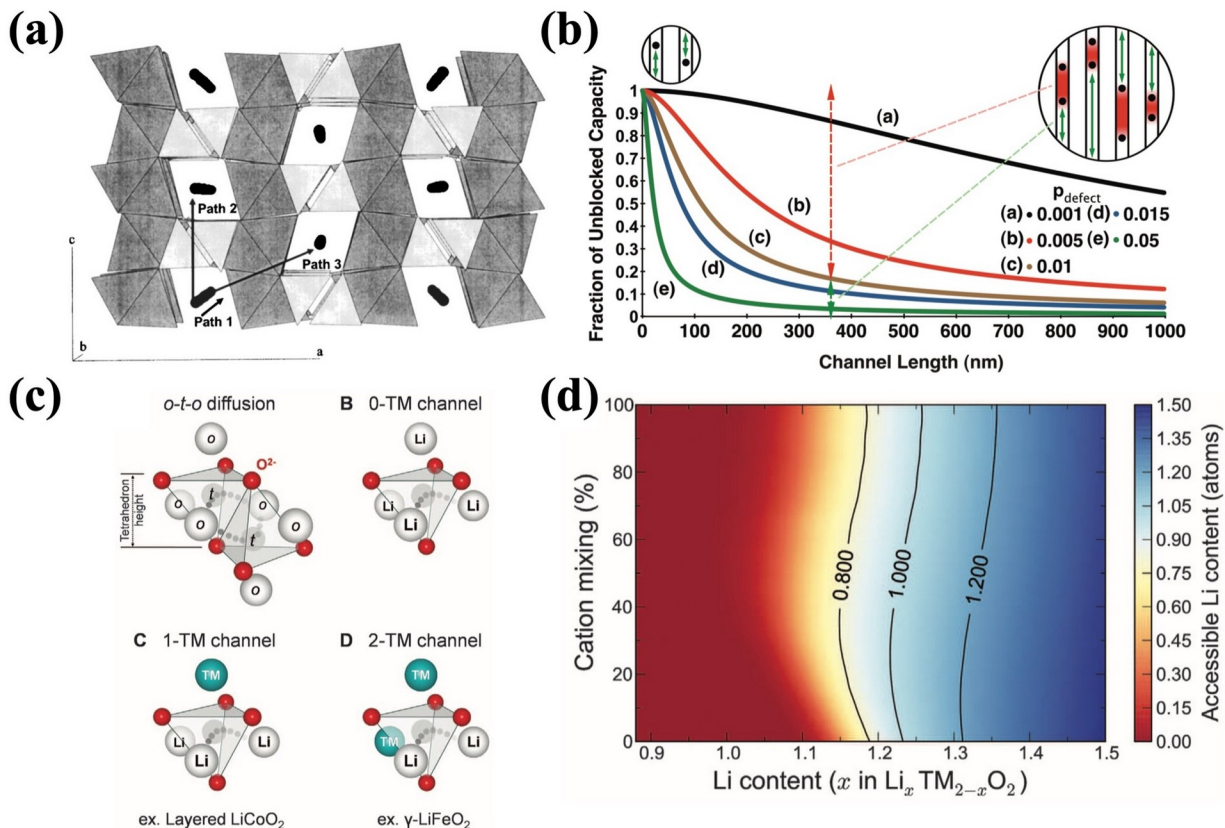


Figure 2. (a) Lithium migration pathways in olivine LiMPO₄. Republished with permission from ²⁴. Copyright 2003 The Electrochemical Society. (b) Expected unblocked capacity as a function of Li-ion channel length for various defect concentrations in LiFePO₄. Reprinted (adapted) with permission from ³² Copyright 2010 American Chemical Society. (c) Possible local environments for Li hopping in rocksalt-like Li-TM oxides. (d) Estimated accessible Li content by a percolating network of 0-TM channels in rocksalt-like Li-TM oxides as a function of Li content and cation mixing. Republished with permission from ³³ Copyright 2014 AAAS.

Another innovative example of a multiscale computational approach to probe ion-dynamics in solid-state conductors has been recently provided by Deng *et al.*,³⁸ with investigations on the effect of polyanion mixing on the Na-ion transport properties of Na_{1+x}Zr₂Si_xP_{3-x}O₁₂ (0 ≤ x ≤ 3) NASICON electrolytes. The authors used DFT-calculated NEB migration barriers to build a Local Cluster Expansion (LCE) Hamiltonian, which was then used in kinetic Monte Carlo (kMC) simulations over milliseconds time-scales and nanometers length-scales. These simulations indicated that fast Na-ion transport is favored by a Si-rich local environment due to lower migration energies. They also found that the optimal Na content (and carrier

concentration) is obtained for $x \sim 2.4$, which explains the high Na-conductivity measured experimentally for $\text{Na}_{3.4}\text{Zr}_2\text{Si}_{2.4}\text{P}_{0.6}\text{O}_{12}$.

As shown by the examples above, the link between atomistic QM simulations of battery materials and simulations on a macroscopic scale is provided by statistical approaches that are broadly based on either ensemble averages (MC) or time averages (MD). These often rely on the empirical representation of interatomic potentials or force fields (FF) to limit computational costs while extending the reach of the potential energy surface (PES) sampling. A major problem intrinsic to (semi-)empirical potentials is their lack of generality, which curbs expectations over accuracy and extrapolation capability. Therefore, great research effort has been devoted in the past two decades to developing physically sophisticated FFs able to reproduce charge polarization effects,³⁹⁻⁴¹ as well as complex chemical reactions (e.g., ReaxFF)⁴² driving the dynamic evolution of battery materials,⁴³ with the aim of achieving increasingly better agreement with experimental observations.

A much simpler and more adaptable type of FF is the one calibrated on the fundamental description of structure environments *via* atomic bond lengths and angles, while complex physical and chemical specificities are neglected. Such FFs are applicable across larger chemical spaces and thus serve well purposes of high-throughput materials screening. The bond-valence-sum (BVS) based FF formulated by Adams *et al.* is a prominent example,^{44, 45} being commonly used for the analysis of ion transport pathways and migration barriers. Figure 3a displays the Li migration-energy diagram from the bond-valence site energy landscape calculated for $\text{Li}_5\text{La}_3\text{Ta}_2\text{O}_{12}$; the overall migration barrier for the percolating Li(2)–Li(1)–Li(2) path (<0.4 eV) is very close to that computed via NEB analysis. Along the same line, Kobayashi *et al.*⁴⁶ have proposed empirical FFs for solid-state ionic conductors using radial and angular distribution functions obtained from *ab initio* MD reference data.

Breakthroughs in statistical machine learning (ML), associated with the rise of materials informatics in recent years, have offered a valuable alternative to classical interatomic potentials fitting.⁴⁷⁻⁵³ Generally speaking, ML potentials are trained on QM reference data and used to explore the associated PES at a substantially higher pace but with comparable accuracy.

Emerging applications of ML potentials hold great promise towards the realistic modeling of battery materials and their behaviors.⁵⁴⁻⁵⁷

Amorphous materials are notable case studies due to the high computational cost of simulating long-range disorder and vast accessible stoichiometries. In modeling amorphous Si anodes, Artrith *et al.* performed a thorough and efficient sampling of the amorphous Li_xSi phase space combining a neural network potential (NNP) with a genetic algorithm.⁵⁸ In addition, NNP-assisted lithium transport investigations have revealed a strong inhibitory effect from under-coordinated Si.^{59, 60} Li *et al.* trained a NNP to simulate ion diffusion in amorphous Li_3PO_4 electrolytes and achieved good agreement with experimental activation energies ($\sim 0.55\text{-}0.58$ eV) using structure models of over 1000 atoms (see Figure 3b).⁶¹ Similarly, computational work showing the impact of off-stoichiometry conditions on the Li-ion diffusion in amorphous LiPON electrolytes has benefited from the aid of NNPs in determining low-energy structure models explored with a genetic-algorithm.⁶²

In addition to enabling access to large model systems, ML potentials also allow to extend the timescale of MD diffusivity simulations while keeping *ab initio* level accuracy. This can reduce the often significant discrepancy between conductivities and activation energies calculated for solid-state ionic conductors and those measured experimentally, as was recently demonstrated by Qi *et al.*⁶³ By using moment tensor potentials (MTPs) for MD simulations at least 1ns long and with up to 2376 atoms, the authors calculated room-temperature ionic conductivities for $\text{Li}_{0.33}\text{La}_{0.56}\text{TiO}_3$ (LLTO), Li_3YCl_6 and $\text{Li}_7\text{P}_3\text{S}_{11}$ in excellent agreement with experimental values, and unveiled a low-temperature (400-450K) transition between different diffusive regimes in all three superionic conductors (Figure 3c). Diffusivity simulations on cathode coating materials by Wang *et al.* provide another prominent example of usage of MTP potentials to access long simulations time scales (up to 2 ns).⁶⁴ In this case, the authors adopted a learning-on-the-fly approach based on *ab initio* MD simulations, which has the advantage of reducing the operational overhead by maximizing automation of the ML potential training process. Galvanized by such advantage, optimized workflows for unsupervised, on-the-fly ML force fields generation have been under active development for a few years, particularly within the framework of the Gaussian Process model⁴⁸ coupled with Bayesian inference.^{52, 53, 65-67} Finally, in

closing on the topic of multiscale modeling of battery materials and components, it is worth mentioning that successful ML predictions of macroscopic mechanical and thermal properties have been implemented *via* statistical learning of data from finite-elements simulations.^{68, 69}

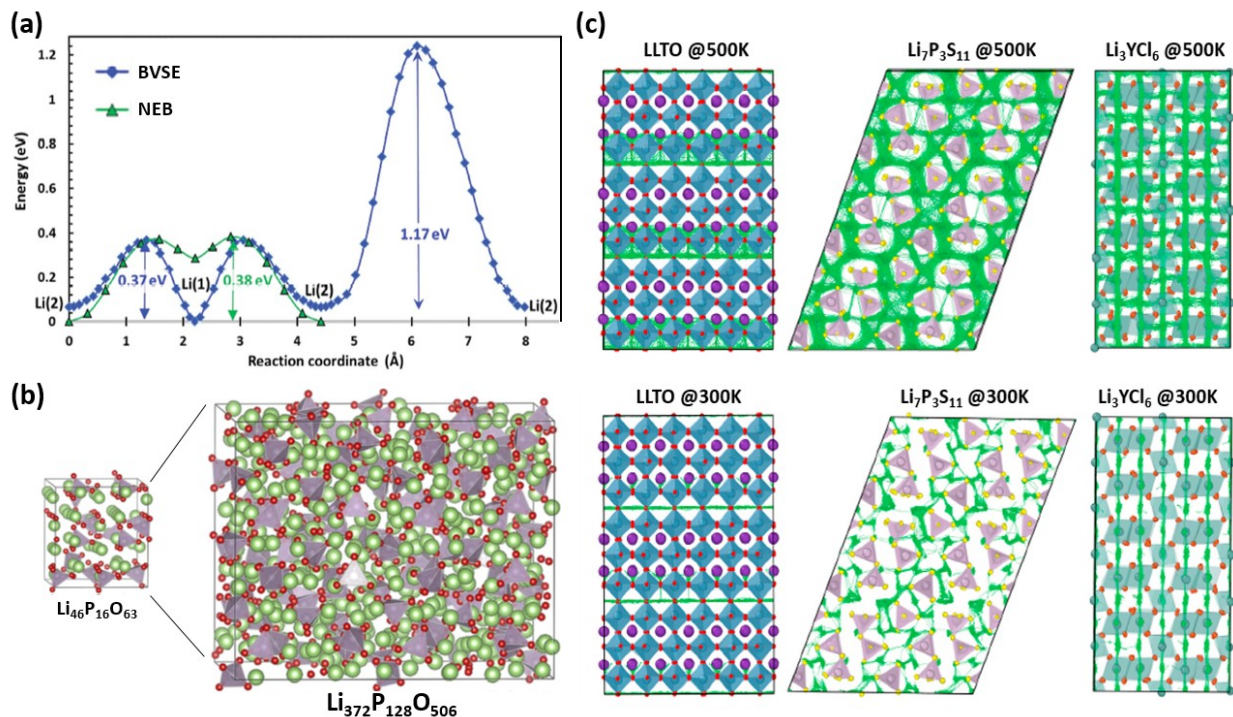


Figure 3. (a) Li migration pathway diagram from the bond-valence site energy (BVSE) landscape calculated for $\text{Li}_5\text{La}_3\text{Ta}_2\text{O}_{12}$. The 3D pathway network is based on hops between Li(1) and Li(2) sites with a barrier <0.4 eV, which is essentially the same as that obtained from NEB calculations. Republished with permission from ⁴⁵ Copyright 2019. International Union of Crystallography. (b) Simulation cells representing amorphous Li_3PO_4 , indicating the step up in system size enabled by moving from DFT to ML potentials. Adapted and reprinted from ⁶¹ Copyright 2017. AIP Publishing. (c) Li trajectories (in green) from MTP-assisted MD simulations of LLTO, Li_3YCl_6 and $\text{Li}_7\text{P}_3\text{S}_{11}$ at room temperature (300 K) and above the transition to high-temperature diffusivity regimes. Reprinted from ⁶³ Copyright 2021. Elsevier.

Progress in Experiments

Along with the efforts for computational approaches to understand the electrochemical reaction mechanisms and their effects on battery performance, there have been significant developments

in experimental characterization techniques to capture the reaction process, with particular attention devoted to *operando* studies (i.e. investigations carried out in real time during battery (dis)charge). Such methods are used to investigate the electrochemical reactions at varied length scales, from the atomic one to the mm-scale of full electrochemical cells. One popular structural characterization tool is X-ray powder diffraction (XRPD). In fact, XRPD exploits constructively scattered X-rays to reconstruct the periodic distribution of atoms into the unit cell of a crystalline material. As such, it can also be used to understand how such structure is modified in electrode materials during cycling. XRPD is now commonly applied *in situ* and *operando* both at synchrotron facilities and on laboratory diffractometers.^{70, 71} For example, XRPD has been used to solve a number of key electrode material-related questions, notably in the case of LiFePO₄ (hereafter, LFP).^{72, 73} LFP is a textbook example of biphasic material, wherein Li deintercalation proceeds via observation of phase-separated LFP + FePO₄. It was later demonstrated *via* XRPD that such biphasic behavior is strongly dependent of various parameters: higher temperature, higher current rate or the use of nanoparticles may all result in a solid solution behavior.⁷⁴⁻⁷⁶ Liu *et al.*, in particular, demonstrated the rate dependence of the LFP reaction pathway (Figure 4a): at low rates Bragg peaks of both LFP and FePO₄ are clearly separated, while at higher rates (>= 10C) diffracted intensity is also present at intermediate positions corresponding to solid solutions Li_xFePO₄.⁷⁶ Hence in the case of LFP, like for several other compounds, XRPD was a crucial tool to spark subsequent studies focused on understanding electrochemical reaction pathways. Very recently, XRPD has also been applied to investigate synthesis reaction mechanisms and thermal stabilities of electrode materials for rechargeable batteries.⁷⁷⁻⁸² A review article in this focus issue highlights the importance of understanding synthesis reaction mechanisms and shows several key examples using *in situ* heating XRPD experiments.⁸³

One important research direction is to combine XRPD with other experimental methods. By doing so, ideally simultaneously or as much as possible under comparable conditions, one can complement the bulk structural information with local, electronic or morphological information. Multi-modal characterization is made possible also by developing sample environments capable of conducting such simultaneous experiments (see as an example Figure 4b),⁸⁴ thereby improving our understanding of the electrochemical reaction mechanisms.⁸⁴⁻⁹⁰ As an example, XRPD has

long been used in combination with XANES (X-ray absorption near edge structure) during charging and discharging of battery materials, to investigate the change in the crystal structure in relation to the varying redox activity of the transition metals. This is particularly useful for example in multi-metal cathodes such as $\text{Li}_x\text{Ni}_y\text{Mn}_z\text{Co}_{1-y-z}\text{O}_2$ (NMC).⁸⁸ XANES was used to prove that in such materials Mn^{4+} is mostly redox inactive, while the oxidation and reduction of Ni and Co occur at different states of charge (SOC). In particular, Ni^{2+} is the main redox active element, especially at voltage cut-off $< 4.5\text{V}$, while the oxidation of Co^{3+} would only occur at higher SOC. Another good example can be found in work by Bianchini *et al.* and by Broux *et al.* on $\text{Na}_3\text{V}_2(\text{PO}_4)_2\text{F}_3$ (NVPF).^{91, 92} The multiple phase transitions driven by strong Na-vacancy orderings as a function of Na concentration in $\text{Na}_{3-x}\text{V}_2(\text{PO}_4)_2\text{F}_3$ were verified by a XRPD study, which also suggested but could not definitively prove V^{4+} disproportionation into $\text{V}^{3+} + \text{V}^{5+}$ in the end member $\text{NaV}_2(\text{PO}_4)_2\text{F}_3$.⁹¹ The XANES technique, further coupled with NMR (Nuclear Magnetic Resonance), finally proved such disproportionation of V^{4+} .⁹²

Beyond XANES, when the local structure needs to be investigated, Extended X-ray Absorption Fine Structure (EXAFS) plays a critical role to understand reaction mechanisms. With proper data reduction and treatment, EXAFS can verify the metal's oxidation state in electrode materials, as well as possible local distortions or deviations from the average bulk crystal structure.⁹³⁻⁹⁵ A particularly interesting example is that of LiNiO_2 and Ni-rich NCM materials, where diffraction experiments always identify an average perfect octahedral environment around Ni^{3+} cations, while EXAFS can prove the existence of a Jahn-Teller distortion at the local scale, whose dynamic, non-cooperative nature was recently suggested.^{96, 97} Being element-specific, XANES and EXAFS in particular can also separate the reaction kinetics in multi-element electrode materials. As shown in Figure 4c, Yu *et al.*, demonstrated using EXAFS that Mn is the rate-limiting redox center, reacting slower than Ni and Co, in Li and Mn-rich NCM material $\text{Li}_{1.2}\text{Ni}_{0.15}\text{Co}_{0.1}\text{Mn}_{0.55}\text{O}_2$.⁹⁸

Another powerful technique to obtain local structural information is Pair Distribution Function (PDF) analysis.^{99, 100} Despite requiring more careful data acquisition (higher Q range and high statistics, careful background correction, etc.), PDF extends the range of applications of XRPD by allowing to characterize not only perfectly crystalline materials, but also those with limited

periodicity, i.e. defective materials, nanocrystalline and even amorphous ones. Recent works have successfully developed *operando* PDF capability using a customized sample environment.^{101, 102} This approach is particularly valuable for the study of conversion and alloying reaction at negative electrodes, where often nanostructures with poor crystallinity are formed,^{103, 104} or for the study of the storage properties of hard carbon anodes.¹⁰⁵ Allan *et al.*, in particular, demonstrated the use of *ex situ* PDF combined with solid-state NMR to identify the intermediate phases occurring during the reaction of Sb used as anode for Na-ion batteries.¹⁰³ Thanks to the use of such techniques, two new intermediate phases were identified, which could be described despite the presence of significant defects (Na vacancies) or being highly amorphous.

An even more detailed and local picture can be obtained by using solid-state NMR. Detailed interpretation of NMR spectra and their use in combination with multiple other scattering techniques has been pioneered by the Grey group and is now an established approach towards a full structural and electronic understanding of electrode materials.^{106, 107} As an example, an *operando* Na-NMR study showed that local environments near Na change significantly as a function of the sodiation level in a Sn anode (Figure 4d).¹⁰⁴ Combined with PDF analysis and DFT computations, Stratford *et al.* could successfully demonstrate the sodiation process in a Sn anode. Recently, various other techniques relying on magnetic properties (magnetometry, EPR) are being developed for the study of electronic properties of materials, even towards *operando* studies.¹⁰⁸⁻¹¹⁰

A thorough understanding of the bulk crystal, its electronic structure, and its defects, are of key importance to develop electrode materials, as well as to build models for simulations that represent realistic samples. Nonetheless, these properties often do not directly correlate with the electrochemical performance of the materials. In fact, various factors, including the materials surface structure, surface impurities, metal dissolutions, cathode-electrolyte interphase (CEI) formation,¹¹¹⁻¹¹³ play a major role in determining the electrochemical performance in terms of both first cycle capacity, as well as capacity evolution over cycling and degradation mechanisms. For the study of the surface structure of electrode materials, XAS with soft X-Rays is often employed. By varying the detection mode from Fluorescence Yield (FY, a few hundred nm probed depth) to Total Electron Yield (TEY, only 5-10 nm) to Auger Yield (AY, 2-5 nm) one

can, at the same time, get information about the bulk, near surface and pure surface electronic structures.^{114, 115} By doing so, one can for example clearly distinguish the more reduced Ni oxidation state at the surface of LiNiO₂ and Ni-rich cathode materials, as compared to the bulk oxidation state. This can also be confirmed by electron microscopy techniques, where the surface structure can be observed to evolve from a layered to a rock salt-like structure upon long-term cycling.¹¹⁶⁻¹¹⁸ XPS is also a sensitive technique to determine the nature of the chemical species present on the surface in the pristine state, as well as evolved during cycling.^{119, 120} At synchrotron facilities, Hard X-ray Photoelectron Spectroscopy (HAXPES) can also be employed to tune the incident photon energy and hence vary the probed depth into the materials.¹²¹ For example, Assat *et al.* used HAXPES to prove that in Li- and Mn-rich NCM materials (Li_{1.2}Ni_{0.13}Mn_{0.54}Co_{0.13}O₂), anionic redox does not only contribute to the activation cycle(s), but rather reversibly persists in the material's bulk after several tens of cycles.¹²¹ However, such anionic redox reactions are not fully reversible. The irreversible anion oxidation often leads to degradation of the electrode materials, which is often correlated with gas evolution from the lattice.¹²² Differential electrochemical mass spectrometry (DEMS) studies are particularly powerful to understand such a degradation mode involving gas evolution. For example, Lee *et al.* clearly showed how O₂ and CO₂ release at the end of charge in disordered rock salt cathode materials could be quantified by DEMS (Figure 4e).¹²² Fluorination was also demonstrated as a viable route to mitigate such gas release. A review article by Dreyer *et al.* in this focus issue provides a comprehensive overview on the gas evolution in battery systems.¹³ The DEMS technique is even more relevant when investigating Li-oxygen (or Li-air) batteries, because the major reaction products of those battery systems are gas species. The work from Bryan's group in this focus issue uses DEMS to demonstrate that nature of carbon electrode and charging protocol are key parameters to optimize Li-air battery performance.¹²

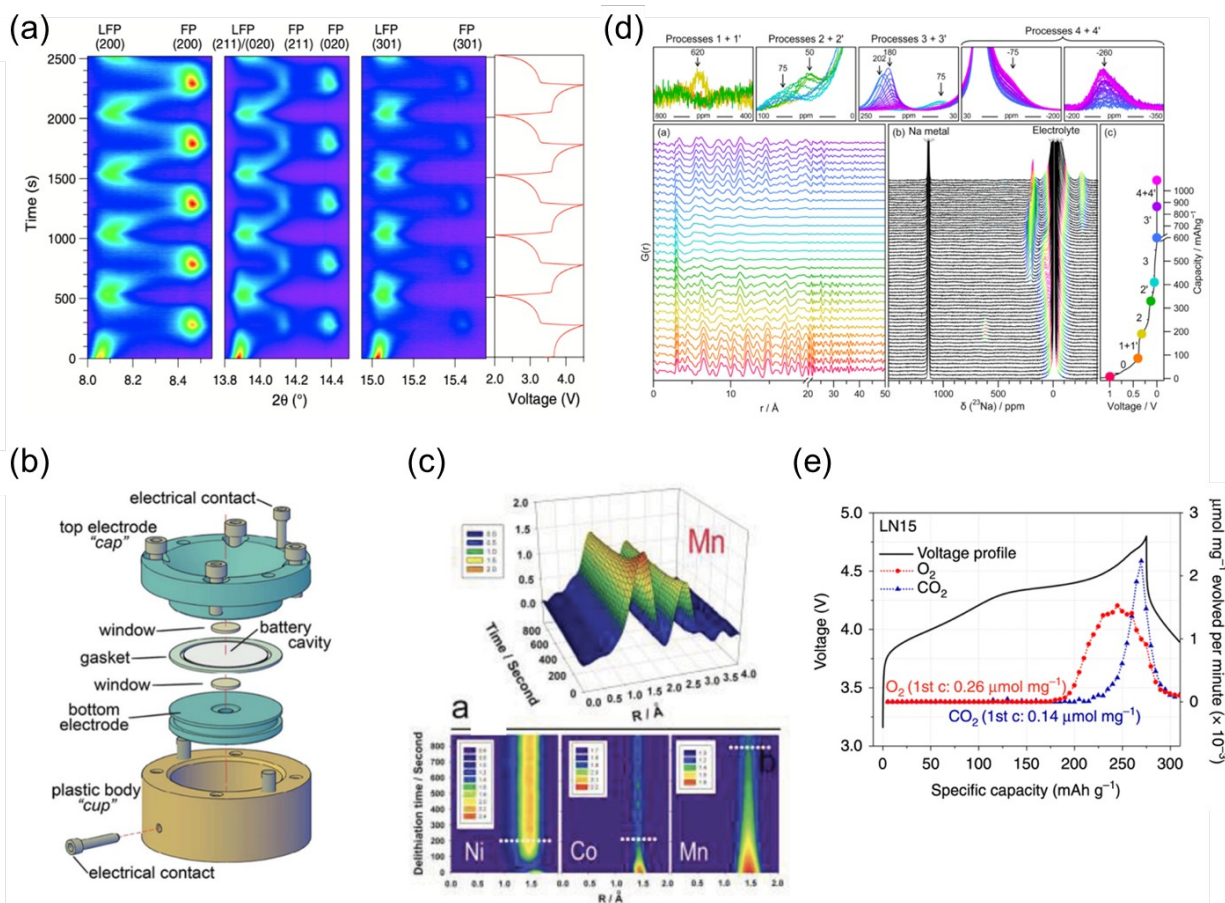


Figure 4. Atomic scale characterization techniques for battery electrode materials. (a) Contour plots of *in situ* (*operando*) XRPD patterns acquired during the first five charge-discharge cycles of LFP at 10C rate. The corresponding voltage curve is plotted to the right. Reproduced from ⁷⁶ Copyright 2014. AAAS (b) An exploded representation of the AMPIX cell, suitable for a broad range of synchrotron-based X-ray scattering and spectroscopic measurements. Reproduced from ⁸⁴ Copyright 2012. International Union of Crystallography. (c) 5 V constant voltage charging applied to the $\text{Li}_{1.2}\text{Ni}_{0.15}\text{Co}_{0.1}\text{Mn}_{0.55}\text{O}_2$ electrode. Ni, Co, Mn reacted simultaneously, which was recorded using a time-resolved XAS technique. At the top, the Fourier transformed Mn K-edge spectra is shown, at the bottom, a projection view of the Ni–O, Co–O, and Mn–O peak magnitudes of the Fourier transformed K-edge spectra as functions of charging time. Reproduced from ⁹⁸ Copyright 2014. John Wiley & Sons, Inc. (d) Operando measurements for electrochemical cells with sodium metal and tin electrodes discharged at C/30 rate. On the left, selected PDFs obtained during the first discharge are vertically offset in time; the colors correspond to the points shown on the electrochemical curve. On the right, ^{23}Na NMR spectra obtained during the first discharge, aligned with the corresponding electrochemistry. Selected regions are highlighted above, where the colors now correspond to the points shown on the electrochemical curve. Reproduced from ¹⁰⁴ Copyright 2017 under a the Creative Commons CC BY license, American Chemical Society. (e) Differential electrochemical mass spectrometry (DEMS) study of $\text{Li}_{1.15}\text{Ni}_{0.375}\text{Ti}_{0.375}\text{Mo}_{0.1}\text{O}_2$ (LN15). Voltage profiles (black solid) of LN15 when

charged to 4.8 V and discharged to 1.5 V at 20 mA g⁻¹, along with the DEMS results on O₂ (red circle) and CO₂ (blue triangle). Reproduced with permission from ¹²² Copyright 2017 under a the Creative Commons CC BY license.

The performance of rechargeable batteries is determined by not only the electrochemical reactions occurring at atomic- and nanometric-scales, but also by structural and compositional changes at microscopic-scales. We will highlight here why characterization at microscopic scales is important to understand the electrochemical reaction mechanisms in rechargeable batteries. Phase separation in a particle upon Li intercalation leads to mechanical strain and may result in fracture of the electrode materials after repeated charging-discharging cycles. Lim *et al.* leveraged spatially resolved *operando* scanning transmission X-ray microscopy (STXM) to track the Li insertion mechanisms by monitoring the valence state of Fe in Li_xFePO₄ at various discharging rates.¹²³ By using a microfluidic electrochemical cell, they could image the Li composition of around 30 single Li_xFePO₄ particles while these are charged and discharged in a liquid electrolyte. They found that the Li-rich (Fe²⁺) and Li-poor (Fe³⁺) regions are separated in a single Li_xFePO₄ particle during discharging at a relatively low current rate (0.2 C) as shown in Figure 5a. In contrast, at a relatively high current rate (2 C), uniform Li intercalation in Li_xFePO₄ is observed without obvious phase separation. The authors claimed that the compositional uniformity within particles minimizes mechanical stress and would show improved cycling stability. A very recent study by the Tang group also investigated the electrochemical reaction mechanisms of Li_xFePO₄ with *ex situ* 3D XANES measurements and *operando* 2D XANES mapping combined with phase-field simulations.¹²⁴ They reported that the Li_xFePO₄ phase exhibits 1D growth behavior in secondary particles and forms rate-independent filament-like domains with the average diameter smaller than the primary particle size. According to their analysis, 1D growth of Li_xFePO₄ phase is attributable to the coherency stress, resulting from the lattice misfit between Li-poor and Li-rich domains. However, their observations are mainly limited to the equilibrium states of Li_xFePO₄ because they used *ex situ* 3D imaging. A recent study by Özdogru *et al.* discovers rate-dependent electrochemical strain changes in LiFePO₄ and NaFePO₄ cathodes, published in this focus issue.¹²⁵ In their experiments, larger strain evolution was recorded at faster charging/discharging rates. In addition, under the pulsed current charging/

discharging conditions, the strain change associated with phase evolutions is delayed at faster rates.

The varying unit cell volume of the electrochemically active material during charging and discharging is one major problem that is responsible for capacity degradation. This issue is particularly critical when the electrode material suffers from a large volume change as is the case for elements alloying with Li (e.g. Sn, Si, etc)^{126, 127} or reacting via conversion reactions (Co_3O_4 , Mn_3O_4 , Fe_2O_3 , etc).¹²⁸⁻¹³⁰ For such compounds, transmission X-ray microscopy (TXM) plays an important role in understanding the effect of volume change on cycling stability and in guiding strategies to mitigate volume expansion upon discharging. For example, the Tolbert group utilized *operando* TXM to investigate the mechanisms that govern the improved cyclability of nanoporous Sn compared to bulk Sn anodes (Figure 5b).¹³¹ They developed and used X-ray-transparent electrochemical cells to monitor morphological changes upon charging and discharging in Li metal cells. They found that the dense Sn anode suffers from a very large volume expansion (~260%) upon discharging, which leads to crack formation in the Sn particles. In contrast, a significantly smaller volume expansion (~30 %) is observed during lithiation in negative electrodes containing porous Sn nanoparticles. In the latter case, the pores volume can accommodate the volume change of the Sn active material during repeated cycling. The main limitation of these 2D TXM images is that the exact pore size and shape cannot yet be determined.

Optical microscopy (OM) is another powerful tool to investigate microstructure evolutions in rechargeable batteries, especially for the materials that have color changes depending on states of charging. One good example is a lithium-sulfur battery. Sun *et al.* investigated the formation of soluble polysulfides and their temporal and spatial distribution over charging and discharging using an *operando* OM technique.¹³² Because the soluble polysulfides have a yellow color in nature, OM can easily capture the formation of polysulfides during battery operations. They provided direct visualization of the shuttle effect of polysulfides. Their observations clearly show the color gradations where cathode-side has a darker color than anode-side. By developing sulfur-poly(3,4-ethylenedioxythiophene) (PEDOT) composite and using a functional Nafion modified separator, they could mitigate the dissolution of polysulfides and shuttle effect, which

are detrimental for cycling stability. Lithiation in graphite is another good test case to study with OM because graphite color varies depending on the state of charge.¹³³ Kang *et al.* investigated the lithiation and delithiation kinetics in graphite with liquid electrolytes using *operando* OM where they discovered different charge and discharge kinetics dependent on the spatial distribution of the Li concentration within the electrode.¹³³ Later, lithiation behaviors in graphite with a solid-state electrolyte were studied by the Dasgupta group.¹³⁴ Without well interconnected solid-state electrolyte domains with the graphite, a strong color gradient from the solid-state electrolyte side to the current collector side is found, indicating non-homogenous lithiation in graphite electrode as shown in Figure 5c. In contrast, homogeneous lithiation is observed when graphite and solid-state electrolyte have good interconnectivity. These results indicate that there is a critical role of microstructure design for composite electrodes for solid-state batteries. Similarly, a recent work by Merryweather *et al.* developed optical interferometric scattering microscopy (iSCAT) and investigated lithiation dynamics in a single particle of Li_xCoO_2 under varied current rates.¹³⁵

Focused ion beam-scanning electron microscope (FIB-SEM) tomography with nanoscale resolution can be used to peek inside a full battery and reconstruct 3D images. Tan *et al.* recently investigated the composite electrode morphology change in a solid-state battery before and after electrochemical cycling.¹³⁶ Their tomography results showed that voids and cracks form near the cathode particles, which lead to contact loss between cathode active material and solid-state electrolyte after repeated cycling (Figure 5d). While the large external pressure (300 MPa) after the cycling could recover some amounts of lost capacity, the study highlights the importance of engineering mechanically stable electrode composite in solid-state batteries. FIB-SEM tomography is a powerful tool to investigate the structure evolution inside the battery cells, yet this method is destructive, hence *operando* characterization is not available. In addition, beam damages during the FIB process must be minimized.

To overcome the limitations of FIB-SEM tomography, several advanced techniques have been introduced. X-ray-based characterization can lead to non-destructive investigation inside the cell while the battery operates. For example, Müller *et al.* utilized X-ray radiography combined with a force sensor, temperature sensors, and electrochemical impedance spectroscopy (EIS) to

understand electrochemical reaction mechanisms of Li/S batteries with a monolayer pouch cell.¹³⁷ Their multimodal characterization correlates the morphology evolutions of solid sulfur (S) and lithium sulfide (Li₂S) with resistance of the cells and temperature distributions. The authors claimed that the lowering viscosity of the liquid electrolyte by the formation of solid phases results in the solution resistance drop. In addition, it is likely that the temperature change is determined by Joule heating as the temperature change coincides with solution resistance of the cell. The authors suggested another possibility, namely that the temperature change is affected by an endothermic sulfur crystallization and exothermic dissolution process. A key advantage of X-ray tomography (XRT) is the fact that it can construct 3D images without opening the cell. A recent work led by Otoyama is a good example.¹³⁸ Using *operando* X-ray computed tomography (X-ray CT), crack formation inside a solid-state electrolyte is visualized during battery operation as represented in Figure 5e. The authors proposed that the primary cause of short-circuiting in the solid-state battery using sulfide electrolytes is the chemical reaction between the sulfide solid electrolyte and Li metal. They claimed that the sulfide electrolyte expands during the decomposition when it meets Li metal and forms small cracks. Then, Li metal can penetrate the small cracks to form new interfaces with the sulfide solid electrolyte. Such a combination of reduction–expansion–cracking of sulfide solid electrolyte is repeated and, eventually, large cracks form and Li metal forms inside the large cracks, which causes short-circuiting. There are other advanced characterization techniques that are non-destructive and can be done *operando*: such as acoustic emission,¹³⁹ ultrasound^{140, 141} and thermal waves characterization.¹⁴² These techniques can scan large areas and even practical full cell dimensions during battery operation. Operando ultrasound characterization typically studies cell-level phase behaviors of electrode materials because ultrasound is sensitive to the density of the materials and the electrode material expands and shrinks upon lithiation and/or delithiation.^{140, 141} A good example is shown in Figure 5f. A recently developed thermal wave-based analysis technique can track the Li concentration in the electrode based on the calibrated relationship between the thermal conductivity and the amount of intercalated Li ions in the electrode.¹⁴²

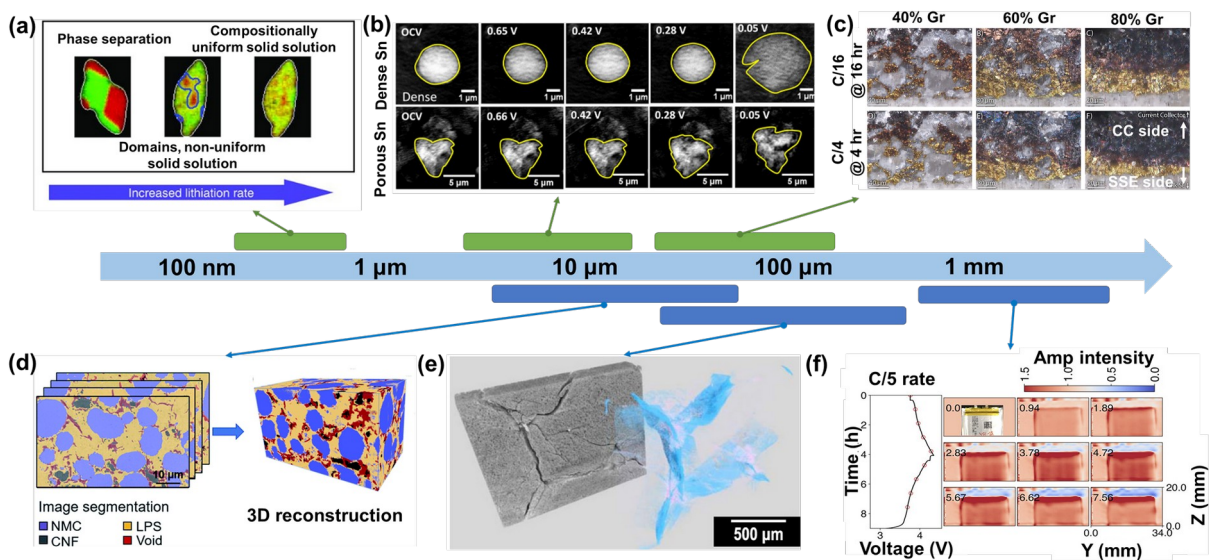


Figure 5. Various micro-scale characterization techniques. (a) Scheme of the Li insertion pathway as a function of the lithiation rate in Li_xFePO_4 . Reproduced with permission from ¹²³ Copyright 2016 American Association for the Advancement of Science. (b) Absorption images of dense and nanoporous tin collected in an X-ray transparent pouch cell using a transmission X-ray microscope operating at 8.95 keV. Reproduced with permission from ¹³¹ Copyright 2017 American Chemical Society. (c) Cross section snapshots of OM in graphite anode with varied graphite and solid electrolyte mixing ratios at C/16 and C/4 rates, taken after 16 and 4 h of lithiation, respectively. Reproduced with permission from ¹³⁴ Copyright 2021 American Chemical Society. (d) Reconstructed 3D volume of the cathode composite in solid state batteries. Reproduced with permission from ¹³⁶ Copyright 2020 under a Creative Commons Attribution-NonCommercial 3.0 Unported Licence. (e) 3D rendered image of the Li_3PS_4 pellet after the galvanostatic cycling test, where cracks and low-density areas are shaded blue and pink,

respectively. Reproduced with permission from ¹⁴⁰ Copyright 2021 American Chemical Society. (f) *Operando* amplitude scanning. C/5 constant current cycle for 400 mAh LiCoO₂/graphite pouch cell. Reproduced with permission from ¹⁴² Copyright 2021 American Chemical Society.

Discussion

While technological advancements and supportive governmental policies are stimulating the transition to renewable energy sources, researchers are challenged by durability and safety concerns around energy storage devices. LIBs and beyond LIBs systems are currently at the center of great research efforts to control the underpinning electrochemical processes and minimize irreversible materials degradation that may ultimately jeopardize the device performance. Multi-scale analyses, including both experiments and simulations, are essential for this purpose, being able to tie observed macroscopic behaviors to the physico-chemical phenomena occurring at the nano- and microscopic level. In this work, we offered an overview of the main experimental and computational methods that are currently being used (or developed) across multiple length and time scales for the exhaustive characterization of battery materials and components.

On the computational side, statistical approaches at the frontier between physics and learning theory are bridging the gap between atomistic quantum-mechanics and continuum-level finite-elements modeling. Probabilistic frameworks are essential to provide quantitative estimates of the detectable outcomes of atomic-scale processes, such as defects formation or ionic migration. This is the case, for example, of Lee *et al.*'s work on DRX cathodes,³³ where MC simulations were used to calculate the probability of Li percolation throughout the material as a function of the Li content. In addition, in the past decade or so, ML approaches to materials simulations have come forward as a pathway to build accurate interatomic potentials, that is, to establish complex functional relationships between energy and atomic positions without the need to solve the

Schrödinger equation. Length- and time-boundaries of traditional quantum-mechanics are thus being pushed forward, as was recently demonstrated, e.g., by the report of ML-assisted Li-ion diffusivity simulations performed on systems with over 2000 atoms over nanoseconds-long trajectories.⁶³

On the experimental side, multi-modal characterizations that measure various properties simultaneously or at least measure those properties within a single setup or device, can greatly improve the understanding of the electrochemical reaction mechanisms. In fact, a number of sample environments capable of simultaneous XRD and XAS experiments have been reported,⁸⁴⁻⁸⁶ and several studies demonstrated the power of this method.^{87, 88, 90} In this respect, it is worth to devote more efforts to develop new *operando* cells that can measure multiple characteristics and properties simultaneously.

With the recent advent of solid-state batteries, where solid electrolytes (especially sulfides with high Li-ion conductivity) have been demonstrated to be in most cases unstable in contact with either positive or negative electrodes,¹⁴³ proper determination and quantification of interfacial reaction byproducts has gained increased importance.¹⁴⁴⁻¹⁴⁶ However, characterization of such interphase formation remains challenging because those interphase materials are buried in the solid materials and they are, in many cases, extremely sensitive to air exposure. Advanced characterization techniques such as cryogenic TEM combined with air-free sample preparation and transfer system will be an exciting direction to pursue in this area. Another powerful tool to study interface regions is Time of Flight Secondary Ion Mass Spectrometry (TOF-SIMS), which allows to reconstruct laterally and depth resolved models of the interfaces and their chemical composition.^{147, 148}

Summary

The electrochemical and chemomechanical reactions occurring inside battery materials and cells are often very complex, yet they determine the overall battery performance. Therefore, a detailed understanding of such processes must be developed. This review article provides an overview of recent advances and remaining challenges in computational and experimental approaches to

understand the electrochemical reactions of battery materials spanning from atomic- to macro-scales. In addition, we would like to highlight that our focus issue provides important findings in this area, with the hope to help the battery community further its understanding of complex electrochemical reaction mechanisms within battery materials and electrodes.

Acknowledgements

This work was partially supported by the 2019 Research Fund (1.190150.01) of UNIST.

Conflict of interest.

The authors declare no conflict of interest.

Data availability

Data sharing not applicable to this article as no datasets were generated or analysed during the current study.

References

1. : <https://www.energy.gov/fecm/carbon-negative-shot>.
2. : <https://www.whitehouse.gov/briefing-room/statements-releases/2021/12/08/fact-sheet-president-biden-signs-executive-order-catalyzing-americas-clean-energy-economy-through-federal-sustainability/>.
3. Z. Yang, J. Zhang, M.C.W. Kintner-Meyer, X. Lu, D. Choi, J.P. Lemmon and J. Liu: Electrochemical Energy Storage for Green Grid *Chemical Reviews*. **111**(5), 3577 (2011).
4. Y. Tian, G. Zeng, A. Rutt, T. Shi, H. Kim, J. Wang, J. Koettgen, Y. Sun, B. Ouyang, T. Chen, Z. Lun, Z. Rong, K. Persson and G. Ceder: Promises and Challenges of Next-Generation “Beyond Li-ion” Batteries for Electric Vehicles and Grid Decarbonization *Chemical Reviews*. **121**(3), 1623 (2021).
5. K. Kubota, M. Dahbi, T. Hosaka, S. Kumakura and S. Komaba: Towards K-Ion and Na-Ion Batteries as “Beyond Li-Ion” *The Chemical Record*. **18**(4), 459 (2018).
6. W. Zhang, J. Yin, W. Wang, Z. Bayhan and H.N. Alshareef: Status of rechargeable potassium batteries *Nano Energy*. **83**, 105792 (2021).

7. F. Liu, T. Wang, X. Liu and L.-Z. Fan: Challenges and Recent Progress on Key Materials for Rechargeable Magnesium Batteries *Advanced Energy Materials*. **11**(2), 2000787 (2021).
8. D. Deb and G. Sai Gautam: Critical overview of polyanionic frameworks as positive electrodes for Na-ion batteries *Journal of Materials Research*. (2022).
9. L. Zou, W. Zhao, Z. Liu, H. Jia, J. Zheng, G. Wang, Y. Yang, J.-G. Zhang and C. Wang: Revealing Cycling Rate-Dependent Structure Evolution in Ni-Rich Layered Cathode Materials *ACS Energy Letters*. **3**(10), 2433 (2018).
10. L. Qiu, M. Zhang, Y. Song, Y. Xiao, Z. Wu, W. Xiang, Y. Liu, G. Wang, Y. Sun, J. Zhang, B. Zhang and X. Guo: Recent advance in structure regulation of high-capacity Ni-rich layered oxide cathodes *EcoMat*. **3**(5), e12141 (2021).
11. W. Li, E.M. Erickson and A. Manthiram: High-nickel layered oxide cathodes for lithium-based automotive batteries *Nature Energy*. **5**(1), 26 (2020).
12. E.A. Kedzie, J.E. Nichols and B.D. McCloskey: Effect of charging protocol and carbon electrode selection in Na-O₂ batteries *Journal of Materials Research*. (2022).
13. S.L. Dreyer, A. Kondrakov, J. Janek and T. Brezesinski: In situ analysis of gas evolution in liquid- and solid-electrolyte-based batteries with current and next-generation cathode materials *Journal of Materials Research*. (2022).
14. Y.-W. Byeon and H. Kim: Review on Interface and Interphase Issues in Sulfide Solid-State Electrolytes for All-Solid-State Li-Metal Batteries *Electrochem*. **2**(3), 452 (2021).
15. R. Koerver, I. Aygün, T. Leichtweiß, C. Dietrich, W. Zhang, J.O. Binder, P. Hartmann, W.G. Zeier and J. Janek: Capacity Fade in Solid-State Batteries: Interphase Formation and Chemomechanical Processes in Nickel-Rich Layered Oxide Cathodes and Lithium Thiophosphate Solid Electrolytes *Chemistry of Materials*. **29**(13), 5574 (2017).
16. J.A. Lewis, F.J.Q. Cortes, M.G. Boebinger, J. Tippens, T.S. Marchese, N. Kondekar, X. Liu, M. Chi and M.T. McDowell: Interphase Morphology between a Solid-State Electrolyte and Lithium Controls Cell Failure *ACS Energy Letters*. **4**(2), 591 (2019).
17. F. Fasulo, A. Massaro, A.B. Muñoz-García and M. Pavone: Na uptake at TiO₂ anatase surfaces under electric field control: A first-principles study *Journal of Materials Research*. (2022).
18. T. Shi, Q. Tu, Y. Tian, Y. Xiao, L.J. Miara, O. Kononova and G. Ceder: High Active Material Loading in All-Solid-State Battery Electrode via Particle Size Optimization *Advanced Energy Materials*. **10**(1), 1902881 (2020).
19. Z.-T. Sun and S.-H. Bo: Understanding electro-mechanical-thermal coupling in solid-state lithium metal batteries via phase-field modeling *Journal of Materials Research*. (2022).
20. J.M. Reniers, G. Mulder and D.A. Howey: Review and Performance Comparison of Mechanical-Chemical Degradation Models for Lithium-Ion Batteries *Journal of The Electrochemical Society*. **166**(14), A3189 (2019).
21. C.D. Parke, L. Teo, D.T. Schwartz and V.R. Subramanian: Progress on continuum modeling of lithium-sulfur batteries *Sustainable Energy & Fuels*. **5**(23), 5946 (2021).
22. H. Euchner and A. Groß: Atomistic modeling of Li- and post-Li-ion batteries *Physical Review Materials*. **6**(4), 040302 (2022).
23. L.M. Morgan, M.P. Mercer, A. Bhandari, C. Peng, M.M. Islam, H. Yang, J. Holland, S.W. Coles, R. Sharpe, A. Walsh, B.J. Morgan, D. Kramer, M.S. Islam,

- H.E. Hoster, J.S. Edge and C.-K. Skylaris: Pushing the boundaries of lithium battery research with atomistic modelling on different scales *Progress in Energy*. **4**(1), 012002 (2021).
24. D. Morgan, A. Van der Ven and G. Ceder: Li Conductivity in $\text{Li}_{1+x}\text{MPO}_4$ (M = Mn, Fe, Co, Ni) Olivine Materials *Electrochemical and Solid-State Letters*. **7**(2), A30 (2004).
 25. M.S. Islam, D.J. Driscoll, C.A.J. Fisher and P.R. Slater: Atomic-Scale Investigation of Defects, Dopants, and Lithium Transport in the LiFePO_4 Olivine-Type Battery Material *Chemistry of Materials*. **17**(20), 5085 (2005).
 26. A. Vasileiadis, N.J.J. de Klerk, R.B. Smith, S. Ganapathy, P.P.R.M.L. Harks, M.Z. Bazant and M. Wagemaker: Toward Optimal Performance and In-Depth Understanding of Spinel $\text{Li}_4\text{Ti}_5\text{O}_{12}$ Electrodes through Phase Field Modeling *Advanced Functional Materials*. **28**(16), 1705992 (2018).
 27. K.J. Griffith, I.D. Seymour, M.A. Hope, M.M. Butala, L.K. Lamontagne, M.B. Preefer, C.P. Koçer, G. Henkelman, A.J. Morris, M.J. Cliffe, S.E. Dutton and C.P. Grey: Ionic and Electronic Conduction in TiNb_2O_7 *Journal of the American Chemical Society*. **141**(42), 16706 (2019).
 28. P. Barnes, Y. Zuo, K. Dixon, D. Hou, S. Lee, Z. Ma, J.G. Connell, H. Zhou, C. Deng, K. Smith, E. Gabriel, Y. Liu, O.O. Maryon, P.H. Davis, H. Zhu, Y. Du, J. Qi, Z. Zhu, C. Chen, Z. Zhu, Y. Zhou, P.J. Simmonds, A.E. Briggs, D. Schwartz, S.P. Ong and H. Xiong: Electrochemically induced amorphous-to-rock-salt phase transformation in niobium oxide electrode for Li-ion batteries *Nature Materials*. **21**(7), 795 (2022).
 29. J. Bhattacharya and A. Van der Ven: Phase stability and nondilute Li diffusion in spinel $\text{Li}_{1+x}\text{Ti}_2\text{O}_4$ *Physical Review B*. **81**(10), 104304 (2010).
 30. S.B. Ma, H.J. Kwon, M. Kim, S.-M. Bak, H. Lee, S.N. Ehrlich, J.-J. Cho, D. Im and D.-H. Seo: Mixed Ionic-Electronic Conductor of Perovskite $\text{Li}_x\text{La}_{1-x}\text{MO}_3$ toward Carbon-Free Cathode for Reversible Lithium-Air Batteries *Advanced Energy Materials*. **10**(38), 2001767 (2020).
 31. S. Hao and C. Wolverton: Lithium Transport in Amorphous Al_2O_3 and AlF_3 for Discovery of Battery Coatings *The Journal of Physical Chemistry C*. **117**(16), 8009 (2013).
 32. R. Malik, D. Burch, M. Bazant and G. Ceder: Particle Size Dependence of the Ionic Diffusivity *Nano Letters*. **10**(10), 4123 (2010).
 33. J. Lee, A. Urban, X. Li, D. Su, G. Hautier and G. Ceder: Unlocking the Potential of Cation-Disordered Oxides for Rechargeable Lithium Batteries *Science*. **343**(6170), 519 (2014).
 34. W. Zhang, D.-H. Seo, T. Chen, L. Wu, M. Topsakal, Y. Zhu, D. Lu, G. Ceder and F. Wang: Kinetic pathways of ionic transport in fast-charging lithium titanate *Science*. **367**(6481), 1030 (2020).
 35. D. Sheppard, R. Terrell and G. Henkelman: Optimization methods for finding minimum energy paths *The Journal of Chemical Physics*. **128**(13), 134106 (2008).
 36. S.-i. Nishimura, G. Kobayashi, K. Ohoyama, R. Kanno, M. Yashima and A. Yamada: Experimental visualization of lithium diffusion in LiFePO_4 *Nature Materials*. **7**(9), 707 (2008).
 37. A. Urban, J. Lee and G. Ceder: The Configurational Space of Rocksalt-Type Oxides for High-Capacity Lithium Battery Electrodes *Advanced Energy Materials*. **4**(13), 1400478 (2014).

38. Z. Deng, T.P. Mishra, E. Mahayoni, Q. Ma, A.J.K. Tieu, O. Guillon, J.-N. Chotard, V. Seznec, A.K. Cheetham, C. Masquelier, G.S. Gautam and P. Canepa: Fundamental investigations on the sodium-ion transport properties of mixed polyanion solid-state battery electrolytes *Nature Communications*. **13**(1), 4470 (2022).
39. O.N. Starovoytov: Development of a Polarizable Force Field for Molecular Dynamics Simulations of Lithium-Ion Battery Electrolytes: Sulfone-Based Solvents and Lithium Salts *The Journal of Physical Chemistry B*. **125**(40), 11242 (2021).
40. O. Borodin and G.D. Smith: Development of Many-Body Polarizable Force Fields for Li-Battery Components: 1. Ether, Alkane, and Carbonate-Based Solvents *The Journal of Physical Chemistry B*. **110**(12), 6279 (2006).
41. O. Borodin and G.D. Smith: Development of Many-Body Polarizable Force Fields for Li-Battery Applications: 2. LiTFSI-Doped Oligoether, Polyether, and Carbonate-Based Electrolytes *The Journal of Physical Chemistry B*. **110**(12), 6293 (2006).
42. A.C.T. van Duin, S. Dasgupta, F. Lorant and W.A. Goddard: ReaxFF: A Reactive Force Field for Hydrocarbons *The Journal of Physical Chemistry A*. **105**(41), 9396 (2001).
43. Z. Shi, J. Zhou and R. Li: Application of Reaction Force Field Molecular Dynamics in Lithium Batteries *Frontiers in Chemistry*. **8**, (2021).
44. S. Adams and R.P. Rao: High power lithium ion battery materials by computational design *physica status solidi (a)*. **208**(8), 1746 (2011).
45. H. Chen, L.L. Wong and S. Adams: SoftBV - a software tool for screening the materials genome of inorganic fast ion conductors *Acta Crystallographica Section B*. **75**(1), 18 (2019).
46. R. Kobayashi, Y. Miyaji, K. Nakano and M. Nakayama: High-throughput production of force-fields for solid-state electrolyte materials *APL Materials*. **8**(8), 081111 (2020).
47. J. Behler and M. Parrinello: Generalized Neural-Network Representation of High-Dimensional Potential-Energy Surfaces *Physical Review Letters*. **98**(14), 146401 (2007).
48. A.P. Bartók, M.C. Payne, R. Kondor and G. Csányi: Gaussian Approximation Potentials: The Accuracy of Quantum Mechanics, without the Electrons *Physical Review Letters*. **104**(13), 136403 (2010).
49. A.P. Bartók, R. Kondor and G. Csányi: On representing chemical environments *Physical Review B*. **87**(18), 184115 (2013).
50. A.P. Thompson, L.P. Swiler, C.R. Trott, S.M. Foiles and G.J. Tucker: Spectral neighbor analysis method for automated generation of quantum-accurate interatomic potentials *Journal of Computational Physics*. **285**, 316 (2015).
51. L. Zhang, J. Han, H. Wang, R. Car and W. E: Deep Potential Molecular Dynamics: A Scalable Model with the Accuracy of Quantum Mechanics *Physical Review Letters*. **120**(14), 143001 (2018).
52. R. Jinnouchi, F. Karsai and G. Kresse: On-the-fly machine learning force field generation: Application to melting points *Physical Review B*. **100**(1), 014105 (2019).
53. J. Vandermause, S.B. Torrisi, S. Batzner, Y. Xie, L. Sun, A.M. Kolpak and B. Kozinsky: On-the-fly active learning of interpretable Bayesian force fields for atomistic rare events *npj Computational Materials*. **6**(1), 20 (2020).

54. V.L. Deringer: Modelling and understanding battery materials with machine-learning-driven atomistic simulations *Journal of Physics: Energy*. **2**(4), 041003 (2020).
55. H. Guo, Q. Wang, A. Stuke, A. Urban and N. Artrith: Accelerated Atomistic Modeling of Solid-State Battery Materials With Machine Learning *Frontiers in Energy Research*. **9**, (2021).
56. C.G. Staacke, H.H. Heenen, C. Scheurer, G. Csányi, K. Reuter and J.T. Margraf: On the Role of Long-Range Electrostatics in Machine-Learned Interatomic Potentials for Complex Battery Materials *ACS Applied Energy Materials*. **4**(11), 12562 (2021).
57. C. Ling: A review of the recent progress in battery informatics *npj Computational Materials*. **8**(1), 33 (2022).
58. N. Artrith, A. Urban and G. Ceder: Constructing first-principles phase diagrams of amorphous Li_xSi using machine-learning-assisted sampling with an evolutionary algorithm *The Journal of Chemical Physics*. **148**(24), 241711 (2018).
59. B. Onat, E.D. Cubuk, B.D. Malone and E. Kaxiras: Implanted neural network potentials: Application to Li-Si alloys *Physical Review B*. **97**(9), 094106 (2018).
60. W. Li and Y. Ando: Effect of local structural disorder on lithium diffusion behavior in amorphous silicon *Physical Review Materials*. **4**(4), 045602 (2020).
61. W. Li, Y. Ando, E. Minamitani and S. Watanabe: Study of Li atom diffusion in amorphous Li_3PO_4 with neural network potential *The Journal of Chemical Physics*. **147**(21), 214106 (2017).
62. V. Lacivita, N. Artrith and G. Ceder: Structural and Compositional Factors That Control the Li-Ion Conductivity in LiPON Electrolytes *Chemistry of Materials*. **30**(20), 7077 (2018).
63. J. Qi, S. Banerjee, Y. Zuo, C. Chen, Z. Zhu, M.L. Holekevi Chandrappa, X. Li and S.P. Ong: Bridging the gap between simulated and experimental ionic conductivities in lithium superionic conductors *Materials Today Physics*. **21**, 100463 (2021).
64. C. Wang, K. Aoyagi, P. Wisesa and T. Mueller: Lithium Ion Conduction in Cathode Coating Materials from On-the-Fly Machine Learning *Chemistry of Materials*. **32**(9), 3741 (2020).
65. R. Jinnouchi, K. Miwa, F. Karsai, G. Kresse and R. Asahi: On-the-Fly Active Learning of Interatomic Potentials for Large-Scale Atomistic Simulations *The Journal of Physical Chemistry Letters*. **11**(17), 6946 (2020).
66. Y. Xie, J. Vandermause, L. Sun, A. Cepellotti and B. Kozinsky: Bayesian force fields from active learning for simulation of inter-dimensional transformation of stanene *npj Computational Materials*. **7**(1), 40 (2021).
67. Y. Xie, J. Vandermause, S. Ramakers, N.H. Protik, A. Johansson and B. Kozinsky: Uncertainty-aware molecular dynamics from Bayesian active learning: Phase Transformations and Thermal Transport in SiC *arXiv preprint arXiv:2203.03824*. (2022).
68. D. Reimann, K. Nidadavolu, H. ul Hassan, N. Vajragupta, T. Glasmachers, P. Junker and A. Hartmaier: Modeling Macroscopic Material Behavior With Machine Learning Algorithms Trained by Micromechanical Simulations *Frontiers in Materials*. **6**, (2019).

69. F. Kolodziejczyk, B. Mortazavi, T. Rabczuk and X. Zhuang: Machine learning assisted multiscale modeling of composite phase change materials for Li-ion batteries' thermal management *International Journal of Heat and Mass Transfer*. **172**, 121199 (2021).
70. F. Lin, Y. Liu, X. Yu, L. Cheng, A. Singer, O.G. Shpyrko, H.L. Xin, N. Tamura, C. Tian, T.-C. Weng, X.-Q. Yang, Y.S. Meng, D. Nordlund, W. Yang and M.M. Doeff: Synchrotron X-ray Analytical Techniques for Studying Materials Electrochemistry in Rechargeable Batteries *Chemical Reviews*. **117**(21), 13123 (2017).
71. M. Morcrette, Y. Chabre, G. Vaughan, G. Amatucci, J.B. Leriche, S. Patoux, C. Masquelier and J.M. Tarascon: In situ X-ray diffraction techniques as a powerful tool to study battery electrode materials *Electrochimica Acta*. **47**(19), 3137 (2002).
72. Y. Orikasa, T. Maeda, Y. Koyama, H. Murayama, K. Fukuda, H. Tanida, H. Arai, E. Matsubara, Y. Uchimoto and Z. Ogumi: Transient Phase Change in Two Phase Reaction between LiFePO₄ and FePO₄ under Battery Operation *Chemistry of Materials*. **25**(7), 1032 (2013).
73. N. Sharma, X. Guo, G. Du, Z. Guo, J. Wang, Z. Wang and V.K. Peterson: Direct Evidence of Concurrent Solid-Solution and Two-Phase Reactions and the Nonequilibrium Structural Evolution of LiFePO₄ *Journal of the American Chemical Society*. **134**(18), 7867 (2012).
74. C. Delacourt, P. Poizot, J.-M. Tarascon and C. Masquelier: The existence of a temperature-driven solid solution in Li_xFePO₄ for $0 \leq x \leq 1$ *Nature Materials*. **4**(3), 254 (2005).
75. A. Yamada, H. Koizumi, S.-i. Nishimura, N. Sonoyama, R. Kanno, M. Yonemura, T. Nakamura and Y. Kobayashi: Room-temperature miscibility gap in Li_xFePO₄ *Nature Materials*. **5**(5), 357 (2006).
76. H. Liu, F.C. Strobridge, O.J. Borkiewicz, K.M. Wiaderek, K.W. Chapman, P.J. Chupas and C.P. Grey: Capturing metastable structures during high-rate cycling of LiFePO₄ nanoparticle electrodes *Science*. **344**(6191), 1252817 (2014).
77. J. Zhao, W. Zhang, A. Huq, S.T. Mixture, B. Zhang, S. Guo, L. Wu, Y. Zhu, Z. Chen, K. Amine, F. Pan, J. Bai and F. Wang: In Situ Probing and Synthetic Control of Cationic Ordering in Ni-Rich Layered Oxide Cathodes *Advanced Energy Materials*. **7**(3), 1601266 (2017).
78. M. Bianchini, J. Wang, R.J. Clément, B. Ouyang, P. Xiao, D. Kitchaev, T. Shi, Y. Zhang, Y. Wang, H. Kim, M. Zhang, J. Bai, F. Wang, W. Sun and G. Ceder: The interplay between thermodynamics and kinetics in the solid-state synthesis of layered oxides *Nature Materials*. **19**(10), 1088 (2020).
79. H. Park, H. Park, K. Song, S.H. Song, S. Kang, K.-H. Ko, D. Eum, Y. Jeon, J. Kim, W.M. Seong, H. Kim, J. Park and K. Kang: In situ multiscale probing of the synthesis of a Ni-rich layered oxide cathode reveals reaction heterogeneity driven by competing kinetic pathways *Nature Chemistry*. **14**(6), 614 (2022).
80. Y. Sun, D. Ren, G. Liu, D. Mu, L. Wang, B. Wu, J. Liu, N. Wu and X. He: Correlation between thermal stabilities of nickel-rich cathode materials and battery thermal runaway *International Journal of Energy Research*. **45**(15), 20867 (2021).
81. X. Liu, L. Yin, D. Ren, L. Wang, Y. Ren, W. Xu, S. Lapidus, H. Wang, X. He, Z. Chen, G.-L. Xu, M. Ouyang and K. Amine: In situ observation of thermal-driven

- degradation and safety concerns of lithiated graphite anode *Nature Communications*. **12**(1), 4235 (2021).
82. Y.-Y. Wang, M.-Y. Gao, S. Liu, G.-R. Li and X.-P. Gao: Yttrium Surface Gradient Doping for Enhancing Structure and Thermal Stability of High-Ni Layered Oxide as Cathode for Li-Ion Batteries *ACS Applied Materials & Interfaces*. **13**(6), 7343 (2021).
 83. F.B. Wang, Pallab; Kahvecioglu, Ozge; Pupek, Krzysztof Z.; Bai, Jianming; Srinivasan, Venkat: Process Design for Calcination of Nickel-based Cathode Materials by In Situ Characterization and Multiscale Modeling *Journal of Materials Research*. (2022).
 84. O.J. Borkiewicz, B. Shyam, K.M. Wiaderek, C. Kurtz, P.J. Chupas and K.W. Chapman: The AMPIX electrochemical cell: a versatile apparatus for in situ X-ray scattering and spectroscopic measurements *Journal of Applied Crystallography*. **45**(6), 1261 (2012).
 85. J.B. Leriche, S. Hamelet, J. Shu, M. Morcrette, C. Masquelier, G. Ouvrard, M. Zerrouki, P. Soudan, S. Belin, E. Elkaim and F. Baudalet: An Electrochemical Cell for Operando Study of Lithium Batteries Using Synchrotron Radiation *Journal of The Electrochemical Society*. **157**(5), A606 (2010).
 86. J. Sottmann, R. Homs-Regojo, D.S. Wragg, H. Fjellvag, S. Margadonna and H. Emerich: Versatile electrochemical cell for Li/Na-ion batteries and high-throughput setup for combined operando X-ray diffraction and absorption spectroscopy *Journal of Applied Crystallography*. **49**(6), 1972 (2016).
 87. P. Bleith, W. van Beek, H. Kaiser, P. Novák and C. Villevieille: Simultaneous in Situ X-ray Absorption Spectroscopy and X-ray Diffraction Studies on Battery Materials: The Case of $\text{Fe}_{0.5}\text{TiOPO}_4$ *The Journal of Physical Chemistry C*. **119**(7), 3466 (2015).
 88. P.-Y. Liao, J.-G. Duh, J.-F. Lee and H.-S. Sheu: Structural investigation of $\text{Li}_{1-x}\text{Ni}_{0.5}\text{Co}_{0.25}\text{Mn}_{0.25}\text{O}_2$ by in situ XAS and XRD measurements *Electrochimica Acta*. **53**(4), 1850 (2007).
 89. S. Permien, T. Neumann, S. Indris, G. Neubüser, L. Kienle, A. Fiedler, A.-L. Hansen, D. Gianolio, T. Bredow and W. Bensch: Transition metal cations on the move: simultaneous operando X-ray absorption spectroscopy and X-ray diffraction investigations during Li uptake and release of a $\text{NiFe}_2\text{O}_4/\text{CNT}$ composite *Physical Chemistry Chemical Physics*. **20**(28), 19129 (2018).
 90. J. Sottmann, F.L.M. Bernal, K.V. Yusenko, M. Herrmann, H. Emerich, D.S. Wragg and S. Margadonna: In operando Synchrotron XRD/XAS Investigation of Sodium Insertion into the Prussian Blue Analogue Cathode Material $\text{Na}_{1.32}\text{Mn}[\text{Fe}(\text{CN})_6]_{0.83} \cdot z \text{H}_2\text{O}$ *Electrochimica Acta*. **200**, 305 (2016).
 91. M. Bianchini, F. Fauth, N. Brisset, F. Weill, E. Suard, C. Masquelier and L. Croguennec: Comprehensive Investigation of the $\text{Na}_3\text{V}_2(\text{PO}_4)_2\text{F}_3\text{-NaV}_2(\text{PO}_4)_2\text{F}_3$ System by Operando High Resolution Synchrotron X-ray Diffraction *Chemistry of Materials*. **27**(8), 3009 (2015).
 92. T. Broux, T. Bamine, L. Simonelli, L. Stievano, F. Fauth, M. Ménétrier, D. Carlier, C. Masquelier and L. Croguennec: VIV Disproportionation Upon Sodium Extraction From $\text{Na}_3\text{V}_2(\text{PO}_4)_2\text{F}_3$ Observed by Operando X-ray Absorption Spectroscopy and Solid-State NMR *The Journal of Physical Chemistry C*. **121**(8), 4103 (2017).
 93. L. Wang, A. Dai, W. Xu, S. Lee, W. Cha, R. Harder, T. Liu, Y. Ren, G. Yin, P. Zuo, J. Wang, J. Lu and J. Wang: Structural Distortion Induced by Manganese

- Activation in a Lithium-Rich Layered Cathode *Journal of the American Chemical Society*. **142**(35), 14966 (2020).
94. K.R. Tallman, G.P. Wheeler, C.J. Kern, E. Stavitski, X. Tong, K.J. Takeuchi, A.C. Marschilok, D.C. Bock and E.S. Takeuchi: Nickel-rich Nickel Manganese Cobalt (NMC622) Cathode Lithiation Mechanism and Extended Cycling Effects Using Operando X-ray Absorption Spectroscopy *The Journal of Physical Chemistry C*. **125**(1), 58 (2021).
 95. F. Zhang, S. Lou, S. Li, Z. Yu, Q. Liu, A. Dai, C. Cao, M.F. Toney, M. Ge, X. Xiao, W.-K. Lee, Y. Yao, J. Deng, T. Liu, Y. Tang, G. Yin, J. Lu, D. Su and J. Wang: Surface regulation enables high stability of single-crystal lithium-ion cathodes at high voltage *Nature Communications*. **11**(1), 3050 (2020).
 96. A. Rougier, C. Delmas and A.V. Chadwick: Non-cooperative Jahn-Teller effect in LiNiO₂: An EXAFS study *Solid State Communications*. **94**(2), 123 (1995).
 97. S. Sicolo, M. Mock, M. Bianchini and K. Albe: And Yet It Moves: LiNiO₂, a Dynamic Jahn-Teller System *Chemistry of Materials*. **32**(23), 10096 (2020).
 98. X. Yu, Y. Lyu, L. Gu, H. Wu, S.-M. Bak, Y. Zhou, K. Amine, S.N. Ehrlich, H. Li, K.-W. Nam and X.-Q. Yang: Understanding the Rate Capability of High-Energy-Density Li-Rich Layered Li_{1.2}Ni_{0.15}Co_{0.1}Mn_{0.55}O₂ Cathode Materials *Advanced Energy Materials*. **4**(5), 1300950 (2014).
 99. S.J.L. Billinge and M.G. Kanatzidis: Beyond crystallography: the study of disorder, nanocrystallinity and crystallographically challenged materials with pair distribution functions *Chemical Communications*. (7), 749 (2004).
 100. J. Bréger, K. Kang, J. Cabana, G. Ceder and C.P. Grey: NMR, PDF and RMC study of the positive electrode material Li(Ni_{0.5}Mn_{0.5})O₂ synthesized by ion-exchange methods *Journal of Materials Chemistry*. **17**(30), 3167 (2007).
 101. H. Liu, P.K. Allan, O.J. Borkiewicz, C. Kurtz, C.P. Grey, K.W. Chapman and P.J. Chupas: A radially accessible tubular in situ X-ray cell for spatially resolved operando scattering and spectroscopic studies of electrochemical energy storage devices *Journal of Applied Crystallography*. **49**(5), 1665 (2016).
 102. K.W. Chapman: Emerging operando and x-ray pair distribution function methods for energy materials development *MRS Bulletin*. **41**(3), 231 (2016).
 103. P.K. Allan, J.M. Griffin, A. Darwiche, O.J. Borkiewicz, K.M. Wiaderek, K.W. Chapman, A.J. Morris, P.J. Chupas, L. Monconduit and C.P. Grey: Tracking Sodium-Antimonide Phase Transformations in Sodium-Ion Anodes: Insights from Operando Pair Distribution Function Analysis and Solid-State NMR Spectroscopy *Journal of the American Chemical Society*. **138**(7), 2352 (2016).
 104. J.M. Stratford, M. Mayo, P.K. Allan, O. Pecher, O.J. Borkiewicz, K.M. Wiaderek, K.W. Chapman, C.J. Pickard, A.J. Morris and C.P. Grey: Investigating Sodium Storage Mechanisms in Tin Anodes: A Combined Pair Distribution Function Analysis, Density Functional Theory, and Solid-State NMR Approach *Journal of the American Chemical Society*. **139**(21), 7273 (2017).
 105. J.M. Stratford, P.K. Allan, O. Pecher, P.A. Chater and C.P. Grey: Mechanistic insights into sodium storage in hard carbon anodes using local structure probes *Chemical Communications*. **52**(84), 12430 (2016).
 106. H. Wang, T.K.J. Köster, N.M. Trease, J. Ségalini, P.-L. Taberna, P. Simon, Y. Gogotsi and C.P. Grey: Real-Time NMR Studies of Electrochemical Double-Layer Capacitors *Journal of the American Chemical Society*. **133**(48), 19270 (2011).
 107. O. Pecher, J. Carretero-González, K.J. Griffith and C.P. Grey: Materials' Methods: NMR in Battery Research *Chemistry of Materials*. **29**(1), 213 (2017).

108. R. Stoyanova, S. Ivanova, E. Zhecheva, A. Samoson, S. Simova, P. Tzvetkova and A.-L. Barra: Correlations between lithium local structure and electrochemistry of layered $\text{LiCo}_{1-2x}\text{Ni}_x\text{Mn}_x\text{O}_2$ oxides: ^7Li MAS NMR and EPR studies *Physical Chemistry Chemical Physics*. **16**(6), 2499 (2014).
109. H. Nguyen and R.J. Clément: Rechargeable Batteries from the Perspective of the Electron Spin *ACS Energy Letters*. **5**(12), 3848 (2020).
110. M. Kalapsazova, S. Ivanova, R. Kukeva, S. Simova, S. Wegner, E. Zhecheva and R. Stoyanova: Combined use of EPR and ^{23}Na MAS NMR spectroscopy for assessing the properties of the mixed cobalt-nickel-manganese layers of $\text{P}_3\text{-Na}_y\text{Co}_{1-2x}\text{Ni}_x\text{Mn}_x\text{O}_2$ *Physical Chemistry Chemical Physics*. **19**(39), 27065 (2017).
111. K. Edström, T. Gustafsson and J.O. Thomas: The cathode-electrolyte interface in the Li-ion battery *Electrochimica Acta*. **50**(2), 397 (2004).
112. W.M. Seong, Y. Kim and A. Manthiram: Impact of Residual Lithium on the Adoption of High-Nickel Layered Oxide Cathodes for Lithium-Ion Batteries *Chemistry of Materials*. **32**(22), 9479 (2020).
113. H.Y. Asl and A. Manthiram: Reining in dissolved transition-metal ions *Science*. **369**(6500), 140 (2020).
114. J. Xu, F. Lin, D. Nordlund, E.J. Crumlin, F. Wang, J. Bai, M.M. Doeff and W. Tong: Elucidation of the surface characteristics and electrochemistry of high-performance LiNiO_2 *Chemical Communications*. **52**(22), 4239 (2016).
115. J. Xu, E. Hu, D. Nordlund, A. Mehta, S.N. Ehrlich, X.-Q. Yang and W. Tong: Understanding the Degradation Mechanism of Lithium Nickel Oxide Cathodes for Li-Ion Batteries *ACS Applied Materials & Interfaces*. **8**(46), 31677 (2016).
116. F. Lin, I.M. Markus, D. Nordlund, T.-C. Weng, M.D. Asta, H.L. Xin and M.M. Doeff: Surface reconstruction and chemical evolution of stoichiometric layered cathode materials for lithium-ion batteries *Nature Communications*. **5**(1), 3529 (2014).
117. J. Xu, F. Lin, M.M. Doeff and W. Tong: A review of Ni-based layered oxides for rechargeable Li-ion batteries *Journal of Materials Chemistry A*. **5**(3), 874 (2017).
118. T. Liu, L. Yu, J. Liu, J. Lu, X. Bi, A. Dai, M. Li, M. Li, Z. Hu, L. Ma, D. Luo, J. Zheng, T. Wu, Y. Ren, J. Wen, F. Pan and K. Amine: Understanding Co roles towards developing Co-free Ni-rich cathodes for rechargeable batteries *Nature Energy*. **6**(3), 277 (2021).
119. G. Assat, D. Foix, C. Delacourt, A. Iadecola, R. Dedryvère and J.-M. Tarascon: Fundamental interplay between anionic/cationic redox governing the kinetics and thermodynamics of lithium-rich cathodes *Nature Communications*. **8**(1), 2219 (2017).
120. N. Andreu, D. Flahaut, R. Dedryvère, M. Minvielle, H. Martinez and D. Gonbeau: XPS Investigation of Surface Reactivity of Electrode Materials: Effect of the Transition Metal *ACS Applied Materials & Interfaces*. **7**(12), 6629 (2015).
121. G. Assat, A. Iadecola, D. Foix, R. Dedryvère and J.-M. Tarascon: Direct Quantification of Anionic Redox over Long Cycling of Li-Rich NMC via Hard X-ray Photoemission Spectroscopy *ACS Energy Letters*. **3**(11), 2721 (2018).
122. J. Lee, J.K. Papp, R.J. Clément, S. Sallis, D.-H. Kwon, T. Shi, W. Yang, B.D. McCloskey and G. Ceder: Mitigating oxygen loss to improve the cycling performance of high capacity cation-disordered cathode materials *Nature Communications*. **8**(1), 981 (2017).

123. J. Lim, Y. Li, D.H. Alsem, H. So, S.C. Lee, P. Bai, D.A. Cogswell, X. Liu, N. Jin, Y.-s. Yu, N.J. Salmon, D.A. Shapiro, M.Z. Bazant, T. Tyliszczak and W.C. Chueh: Origin and hysteresis of lithium compositional spatiodynamics within battery primary particles *Science*. **353**(6299), 566 (2016).
124. F. Wang, K. Yang, M. Ge, J. Wang, J. Wang, X. Xiao, W.-K. Lee, L. Li and M. Tang: Reaction Heterogeneity in LiFePO₄ Agglomerates and the Role of Intercalation-Induced Stress *ACS Energy Letters*. **7**(5), 1648 (2022).
125. B. Ozdogru, V. Murugesan and Ö.Ö. Çapraz: Rate-dependent electrochemical strain generation in composite iron phosphate cathodes in Li-ion batteries *Journal of Materials Research*. (2022).
126. Y. Xu, Q. Liu, Y. Zhu, Y. Liu, A. Langrock, M.R. Zachariah and C. Wang: Uniform Nano-Sn/C Composite Anodes for Lithium Ion Batteries *Nano Letters*. **13**(2), 470 (2013).
127. C.K. Chan, H. Peng, G. Liu, K. McIlwrath, X.F. Zhang, R.A. Huggins and Y. Cui: High-performance lithium battery anodes using silicon nanowires *Nature Nanotechnology*. **3**(1), 31 (2008).
128. H. Kim, D.-H. Seo, S.-W. Kim, J. Kim and K. Kang: Highly reversible Co₃O₄/graphene hybrid anode for lithium rechargeable batteries *Carbon*. **49**(1), 326 (2011).
129. H. Kim, S.-W. Kim, J. Hong, Y.-U. Park and K. Kang: Electrochemical and ex-situ analysis on manganese oxide/graphene hybrid anode for lithium rechargeable batteries *Journal of Materials Research*. **26**(20), 2665 (2011).
130. X. Zhu, Y. Zhu, S. Murali, M.D. Stoller and R.S. Ruoff: Nanostructured Reduced Graphene Oxide/Fe₂O₃ Composite As a High-Performance Anode Material for Lithium Ion Batteries *ACS Nano*. **5**(4), 3333 (2011).
131. J.B. Cook, T.C. Lin, E. Detsi, J.N. Weker and S.H. Tolbert: Using X-ray Microscopy To Understand How Nanoporous Materials Can Be Used To Reduce the Large Volume Change in Alloy Anodes *Nano Letters*. **17**(2), 870 (2017).
132. Y. Sun, Z.W. Seh, W. Li, H. Yao, G. Zheng and Y. Cui: In-operando optical imaging of temporal and spatial distribution of polysulfides in lithium-sulfur batteries *Nano Energy*. **11**, 579 (2015).
133. S. Kang, S.J. Yeom and H.-W. Lee: Side-View Operando Optical Microscopy Analysis of a Graphite Anode to Study Its Kinetic Hysteresis *ChemSusChem*. **13**(6), 1480 (2020).
134. A.L. Davis, V. Goel, D.W. Liao, M.N. Main, E. Kazyak, J. Lee, K. Thornton and N.P. Dasgupta: Rate Limitations in Composite Solid-State Battery Electrodes: Revealing Heterogeneity with Operando Microscopy *ACS Energy Letters*. **6**(8), 2993 (2021).
135. A.J. Merryweather, C. Schnedermann, Q. Jacquet, C.P. Grey and A. Rao: Operando optical tracking of single-particle ion dynamics in batteries *Nature*. **594**(7864), 522 (2021).
136. T. Shi, Y.-Q. Zhang, Q. Tu, Y. Wang, M.C. Scott and G. Ceder: Characterization of mechanical degradation in an all-solid-state battery cathode *Journal of Materials Chemistry A*. **8**(34), 17399 (2020).
137. R. Müller, I. Manke, A. Hilger, N. Kardjilov, T. Boenke, F. Reuter, S. Dörfler, T. Abendroth, P. Härtel, H. Althues, S. Kaskel and S. Risse: Operando Radiography and Multimodal Analysis of Lithium-Sulfur Pouch Cells—Electrolyte Dependent Morphology Evolution at the Cathode *Advanced Energy Materials*. **12**(13), 2103432 (2022).

138. M. Otoyama, M. Suyama, C. Hotehama, H. Kowada, Y. Takeda, K. Ito, A. Sakuda, M. Tatsumisago and A. Hayashi: Visualization and Control of Chemically Induced Crack Formation in All-Solid-State Lithium-Metal Batteries with Sulfide Electrolyte *ACS Applied Materials & Interfaces*. **13**(4), 5000 (2021).
139. S. Schweidler, M. Bianchini, P. Hartmann, T. Brezesinski and J. Janek: The Sound of Batteries: An Operando Acoustic Emission Study of the LiNiO₂ Cathode in Li-Ion Cells *Batteries & Supercaps*. **3**(10), 1021 (2020).
140. W. Chang and D. Steingart: Operando 2D Acoustic Characterization of Lithium-Ion Battery Spatial Dynamics *ACS Energy Letters*. **6**(8), 2960 (2021).
141. J.B. Robinson, M. Maier, G. Alster, T. Compton, D.J.L. Brett and P.R. Shearing: Spatially resolved ultrasound diagnostics of Li-ion battery electrodes *Physical Chemistry Chemical Physics*. **21**(12), 6354 (2019).
142. Y. Zeng, D. Chalise, Y. Fu, J. Schaadt, S. Kaur, V. Battaglia, S.D. Lubner and R.S. Prasher: Operando spatial mapping of lithium concentration using thermal-wave sensing *Joule*. **5**(8), 2195 (2021).
143. W.D. Richards, L.J. Miara, Y. Wang, J.C. Kim and G. Ceder: Interface Stability in Solid-State Batteries *Chemistry of Materials*. **28**(1), 266 (2016).
144. J. Auvergniot, A. Cassel, D. Foix, V. Viallet, V. Seznec and R. Dedryvère: Redox activity of argyrodite Li₆PS₅Cl electrolyte in all-solid-state Li-ion battery: An XPS study *Solid State Ionics*. **300**, 78 (2017).
145. Y. Ma, J.H. Teo, D. Kutsche, T. Diemant, F. Strauss, Y. Ma, D. Goonetilleke, J. Janek, M. Bianchini and T. Brezesinski: Cycling Performance and Limitations of LiNiO₂ in Solid-State Batteries *ACS Energy Letters*. **6**(9), 3020 (2021).
146. W. Zhang, F.H. Richter, S.P. Culver, T. Leichtweiss, J.G. Lozano, C. Dietrich, P.G. Bruce, W.G. Zeier and J. Janek: Degradation Mechanisms at the Li₁₀GeP₂S₁₂/LiCoO₂ Cathode Interface in an All-Solid-State Lithium-Ion Battery *ACS Applied Materials & Interfaces*. **10**(26), 22226 (2018).
147. F. Walther, R. Koerver, T. Fuchs, S. Ohno, J. Sann, M. Rohnke, W.G. Zeier and J. Janek: Visualization of the Interfacial Decomposition of Composite Cathodes in Argyrodite-Based All-Solid-State Batteries Using Time-of-Flight Secondary-Ion Mass Spectrometry *Chemistry of Materials*. **31**(10), 3745 (2019).
148. Y. Ma, J.H. Teo, F. Walther, Y. Ma, R. Zhang, A. Mazilkin, Y. Tang, D. Goonetilleke, J. Janek, M. Bianchini and T. Brezesinski: Advanced Nanoparticle Coatings for Stabilizing Layered Ni-Rich Oxide Cathodes in Solid-State Batteries *Advanced Functional Materials*. **32**(23), 2111829 (2022).